An Examination of Radar and Lightning Characteristics of the "Atlanta Tornado" of March 14-15, 2008

John M. Trostel*, Jenny L. Matthews, and Colleen Coyle
Severe Storms Research Center, Georgia Tech Research Institute, Atlanta, Georgia

Nicholas W. S. Demetriades
Vaisala, Inc., Tucson, Arizona

1 INTRODUCTION

On the evening of March 14, 2008, an EF2 tornado swept through the downtown area of Atlanta Georgia. This event was unusual in that it directly impacted the downtown area of a major metropolitan area. The effects of the tornado were immediately broadcast nationwide as the SEC championship quarterfinals were being held in the Georgia Dome which lay just south of the path of the storm. The storm continued through the heart of downtown Atlanta, causing major damage and resulting in one fatality. A second, non-tornadic storm followed the first storm on a slightly more southerly track.

NEXRAD WSR-88D radar data has been examined and compared with Cloud to Ground (CG) and Cloud to Cloud (CC) lightning data obtained from the National Lightning Detection Network (NLDN) for two storms, one tornadic and one non-tornadic that crossed the Atlanta metropolitan during this event. A modified version of the Storm Cell Identification and Tracking (SCIT) algorithm has been used to correlate specific NLDN flashes with each cell. Lightning characteristics such as flash rate, peak current, polarity, and flash type have been examined for both cells.

The general synoptic situation which generated the storm cells is described in Section 2. This includes a short discussion of the surface and upper air maps, as well as the thermodynamic characteristics of the atmosphere. The radar characteristics of the storms are described in Section 3. Data from the National Climate Data Center (NCDC) NEXRAD archives has been examined with both the WDSS-II (Weather Decision Support System – Integrated Information) and the GR2Analyst software packages. Lightning stroke and flash data was obtained for these storms from Vaisala Inc. from the NLDN. This data set is described in Section 4. The SCIT algorithm is briefly described in Section 5, along with the modifications made to the algorithm to enhance it's usefulness with these storm cells. The modified SCIT algorithm allowed the automated association of NLDN flashes with well defined individual storm cells. The results of the NLDN and storm cell association and the differing flash characteristics of each cell are examined in Section 6.

2 SYNOPTIC SUMMARY

The Atlanta Tornado formed under less than ideal conditions. The tornado developed from one of two supercells that formed in northeast Alabama and then moved into northwest Georgia during the evening hours of March 14, 2008. The two supercells, including one which produced an EF2 tornado, formed during the cooler part of Georgia's main severe weather season. Severe thunderstorms that take place during this cooler part of the season or during the November to October cool season display rather different characteristics than storms which form during the main tornado season, from April through June. These cool season storms are found to most likely develop during the late evening (Wasula 2004). These nighttime events are also more likely to exhibit both low convective available potential energy (CAPE) values, <1000 J/kg, and exist in high shear environments with storm relative helicity (SRH) values greater than 200 m^2/s^2 (Guyer and Imy 2006). Due to the differences in parameters between cool and warm season tornado environments, the environment leading to a cool season tornado sometimes can look less threatening than the warm season tornado

* *Corresponding author address*: John M. Trostel, Severe Storms Research Center, Georgia Tech Research Institute, Georgia Institute of Technology, Atlanta, GA 30332-0857; email: john.trostel@gtri.gatech.edu

environment (Davies 2006). These cool season tornadoes can, however, be just as deadly as their warm season counterparts. Therefore, learning how to accurately predict these storms and understanding the associated parameters can be very useful.

The tornado that swept through downtown Atlanta on the evening of March 14, 2008 exhibited many of these cool season characteristics and presented a somewhat subtle synoptic situation. With some of the usual ingredients needed for severe weather in the warm season missing, the Atlanta tornado is better explained using cool season severe weather parameters.

The first clue in determining the circumstances surrounding the development of this tornado was to examine the CAPE values as well as the SRH values. Usually, significantly larger values of CAPE and SRH than were observed are needed to develop tornadic severe weather in the warm season (Davies 2006). Cool season tornadic severe weather, however, can be instigated by the coupling of significantly lower values of CAPE with relatively high SRH values.

Figure 1 displays the Peachtree City, Georgia WFO (KFFC) sounding at 00Z from March 15, 2008. Peachtree City is located about 30 miles south of the metropolitan Atlanta area. The 00Z sounding corresponds to a local time of 8:00pm, about 90 minutes prior to the touchdown of the tornado at 9:38pm. The sounding indicated a modest CAPE value of 1030 J/kg. The 0-3 km SRH values were found to be relatively high at 215 m^2/s^2. Therefore, this situation was characteristic of a cool season storm development with the low, modest CAPE values coupled with the high SRH values.

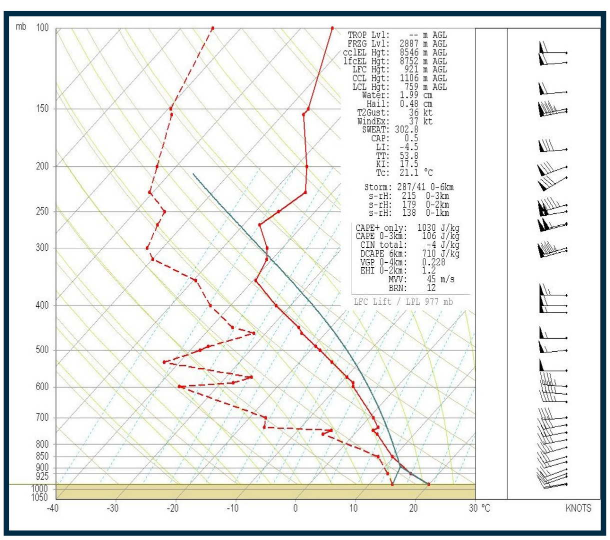

Figure 1: KFFC Sounding for 00Z March 15 2008.

Another informative value to look at is the 0-3 km low-level CAPE. Moderately high and concentrated CAPE values over 100 J/kg in the lower levels is a good indicator of low-level buoyancy and indicates sufficient warm, moist air for tornado development (Guyer and Imy 2006). The 0-3 km CAPE value from the KFFC sounding at 00Z was 106 J/kg. This CAPE value in the low levels confirmed that this tornado has a good source of low level moisture. The fairly low LCL level located at 759 m further indicated warm, moist low levels (Guyer and Imy 2006)

Additional severe weather indices which indicated a marginally severe environment included the Lifted Index (LI) at -4.5 and the SWEAT index of 302.8 (Rauber et al., 2005). A peculiar condition to note is the lack of strong directional shear in the sounding. The KFFC sounding displayed westerly winds throughout the vertical with only changes in wind speeds. These changes were, however, dramatic, with the speed increasing from 30-40 kts in the low levels to over 100 kts at upper levels.

The March 14th 12Z (8am local time) and March 15th 00Z (8pm local time) surface charts as seen in Figure 2 and Figure 3, respectively, set up the synoptic situation just prior to the tornado touchdown. A large low pressure system initially located in the Arkansas – Tennessee area at 12Z moved into the Virginia area by 00Z trailing a cold front.

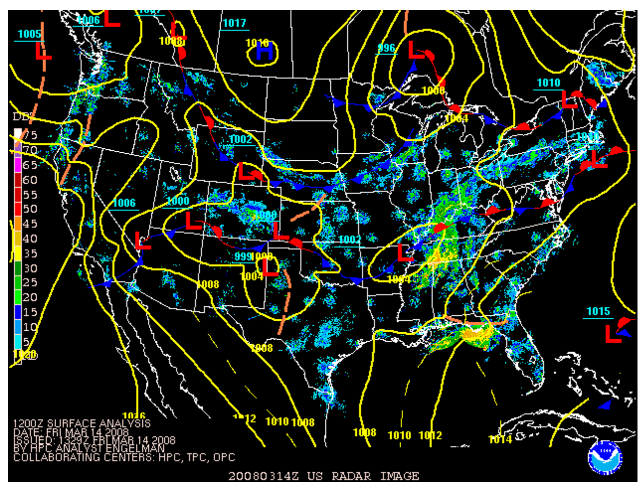

Figure 2. 12Z March 14 2008: Surface Chart

Careful examination of the 12Z chart in Figure 2 shows the two supercells starting to form in extreme eastern Alabama and western Georgia just ahead of the trailing cold front.

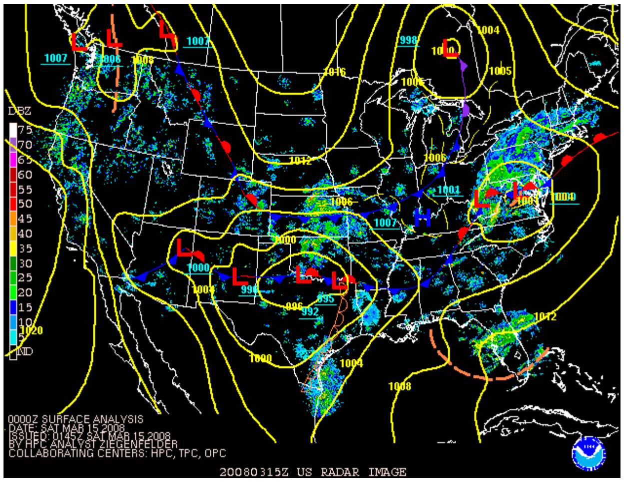

Figure 3. 00Z March 15 2008: Surface Chart

The 500 mb heights and temperature plots for 12Z on the 14th and 00Z on the 15th are presented in Figures 4 and 5 below. Cool season tornadoes are known to exhibit somewhat weak 500mb shortwave troughs as is seen in Figure 4. The deep 500mb troughs that aid in the formation of supercells and tornadoes during the warm season are often absent in the cool season (Guyer and Imy, 2006).

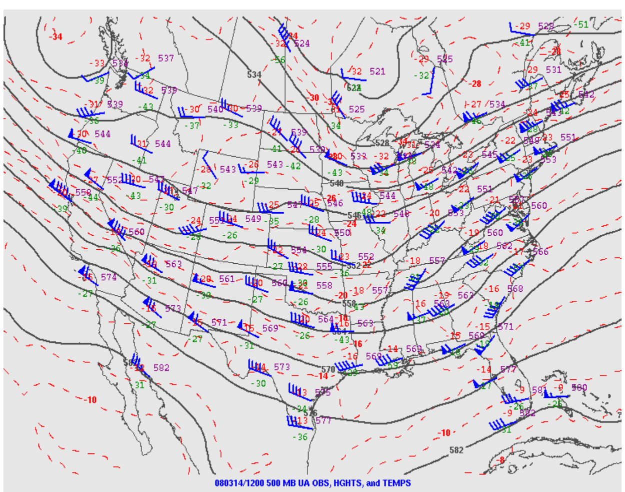

Figure 4. 12Z March 14 2008: 500 mb Chart

Figures 4 and 5 also show a minor shortwave trough moving to the east as well as a strong upper level jet across the gulf states.

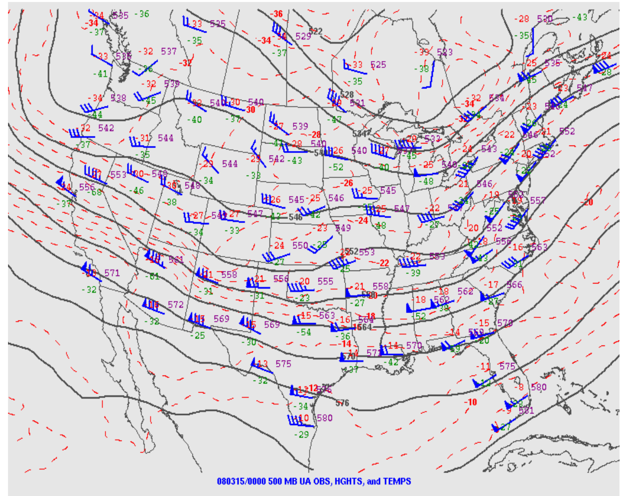

Figure 5. 00Z 15 March 2008: 500 mb Chart

The short wave progression from the Louisiana and Mississippi area into Alabama and Georgia area is even more evident in the 700 mb plots shown in Figures 6 and 7. Also, strong midlevel winds are apparent in both charts over the affected area.

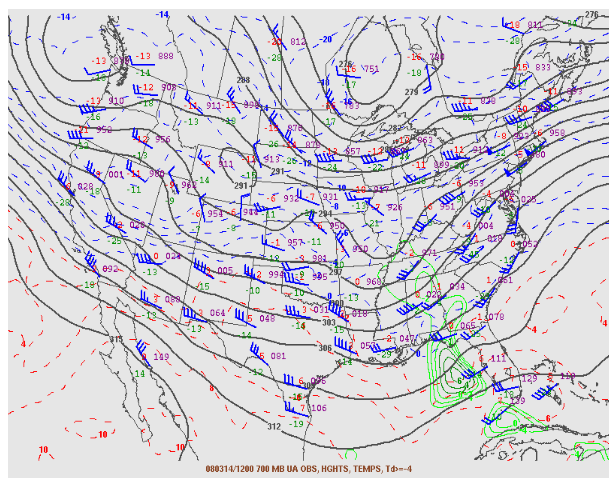

Figure 6. 12Z March 14 2008: 700 mb Chart

Mid level moisture, apparent in the 12Z 700 mb chart, in the Alabama and south Georgia area can be seen to be absent in the 00Z midlevel chart. This drying is reflected in the large extent of dry air shown at midlevels in the KFFC 00Z sounding shown in Figure 1.

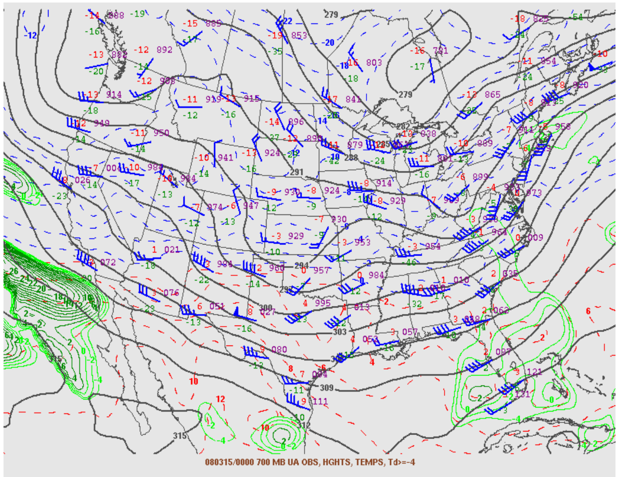

Figure 7. 12Z 15 March 2008: 700 mb Chart

The lower level, 850 mb heights, temperatures and dewpoints are shown for 00Z and 12Z in Figures 8 and 9 below.

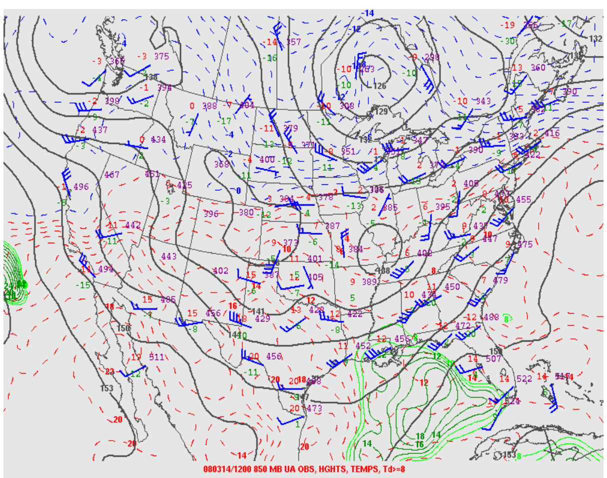

Figure 8. 12Z March 14 2008: 850 mb Chart

Figures 8 and 9 depict a moderately strong subtropical jet with wind speeds of 30 to 35 kts over the area supplying sufficient moisture ahead of the cold front. Comparison of the 12Z and 00Z plots shows a substantial increase in low level moisture ahead of the cold front in the hours prior to initiation of the supercells.

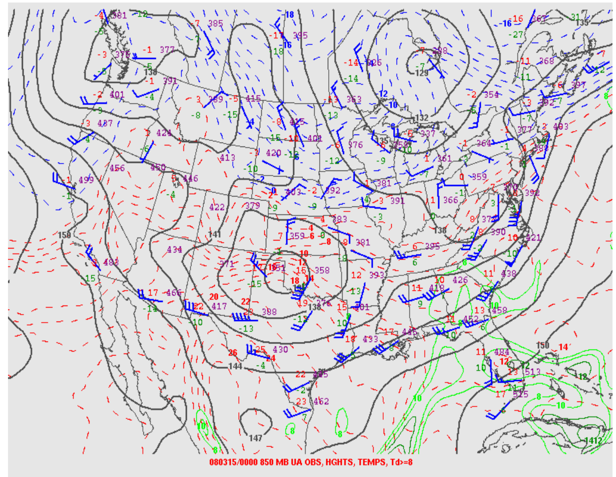

Figure 9. 00Z 15 March 2008: 850 mb Chart

3 RADAR DATA

NEXRAD radar data, obtained from the Level II archives at NCDC, was used to track the supercell movement. Initial observations of the cells movement and development were made using GR2Analyst software.

A plot of storm relative velocity in Figure 10 shows that the two main supercells demonstrated a significant level of low level rotation even as they entered the northwest part of Georgia. Figure 11 depicts the low level (0.5 degree elevation) reflectivity of the lead tornadic supercell just prior to touchdown at 0127Z. The cell shows a pronounced hook and a clear inflow notch. The corresponding plot of low level storm relative velocity, Figure 12, shows a fairly well defined rotational couplet corresponding well to the hook and notch areas.

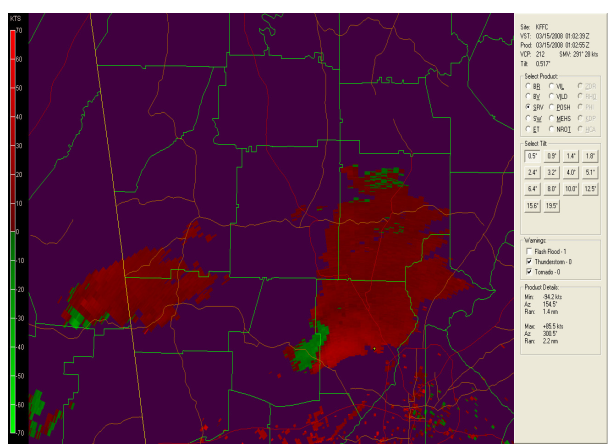

Figure 10. Storm Relative Velocity at 0102Z

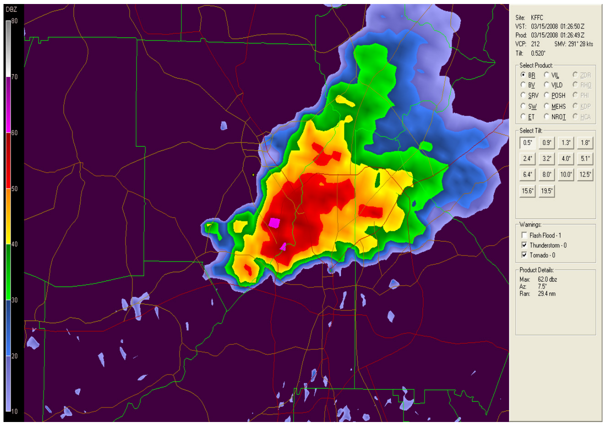

Figure 11. Reflectivity of tornadic cell at 0127Z

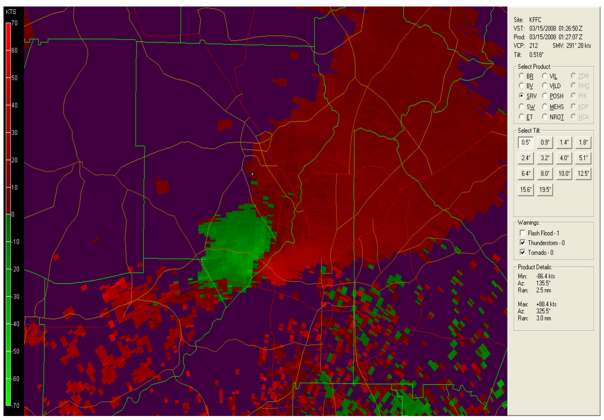

Figure 12. Storm relative velocity of tornadic cell at 0127Z

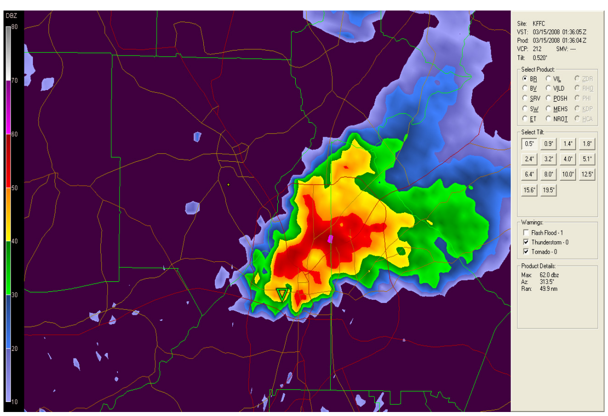

Figure 13. Low level reflectivity and TVS of tornadic cell at 0138Z

Figure 13 shows the low level reflectivity at 0138Z, about 8 minutes after a tornado warning was issued, and just about the time of the first reports of the tornado were received Again, the pronounced inflow region is easily seen just to the right of the TVS symbol, a green triangle, plotted by GR2Analyst.

At 9:40pm, the TVS signature continued to moved eastward through the heart of downtown Atlanta. When the tornado lifted, it had made a path up to 200 yards wide and 6 miles long.

4 NLDN LIGHTNING DATA

Both Cloud to Ground (CG) and Cloud to Cloud (CC) lightning flash and stroke data was acquired from Vaisala's National Lightning Detection Network (NLDN). Data was obtained for the state of Georgia covering the days of March 14th and 15th, 2008.

The NLDN consists of over 100 remote, ground-based IMPACT sensors broadly distributed over the continental United States. These sensors collaboratively detect the location of lightning events using both direction finding (DF) and time of arrival (TOA) methods. Typically between 6 and 8 sensors are used to detect each event.

The data from each IMPACT sensor is collected at the National Collection Center (NCC) located in Tucson, Arizona. At the NCC, the data is analyzed to produce data sets consisting of stroke location, time, polarity, amplitude and type. Additionally, strokes are grouped into flashes based on temporal and spatial constraints.

CG flash detection efficiency with the NLDN approaches 95 percent, with a median location accuracy of 500 meters. CC events, typically one or two per flash, are detected at a lower efficiency, on the order of 10 to 20 percent. In this study, comparisons were typically made between CG and CC rates between different storms. This allows the difference in detection efficiencies to play a lesser role than if the CC and CG rates were compared within a single storm.

5 SCIT MODIFICATIONS AND DATA INTEGRATION

The temporal correlation of lightning and tornadic potential in storm cells has been evaluated using a slightly modified SCIT algorithm associated with the appropriate NLDN data. The basic SCIT algorithm was developed to identify, characterize, and track individual storm cells in NEXRAD data sets (Johnson, et.al., 1998).

One of the features of the original SCIT algorithm was its use of seven different reflectivity thresholds. This study benefited from the use of a smaller set of lower reflectivity thresholds. The use of lower thresholds resulted in identified storm cells containing a larger area. This larger area allowed the inclusion of more lightning strikes for each identified storm. This, in turn, lead to better accuracy in evaluating lightning strike frequency, strength, polarity, and cloud-cloud vs. cloud-ground lightning strikes over time. It also decreased the likelihood that an identified storm cell would be improperly tracked. Although some loss in spatial resolution results from this modification, the corresponding benefit is greater temporal accuracy.

The modified SCIT algorithm was run on quality controlled (QC) reflectivity data output by a neural network in the WDSS-II system (Lakshmanan, et. al., 2007). The use of QC reflectivity data is important because much of the high reflectivity returns that result from non-precipitating targets such as birds, planes, and ground clutter has been removed. Without this removal these non-meteorological targets might be identified as storm cells. The worst case scenario is that such a non-meteorological target is contained in a true storm area. According to the SCIT algorithm, the true storm cell would then be discarded in order to store the higher reflectivity "storm cell." Thus, QC reflectivity not only prevents false storm cells from being detected, but also prevents true storm cells from being thrown away.

5.1 Initial NLDN and NEXRAD Correlation using WDSS-II

The WDSS-II system includes components which allow the user to ingest both NLDN lightning flash data and NEXRAD radar data and to present both of these data sets in a temporally correlated display. An example of the integration of these two data sets for the March 14-15 event is shown in Figure 14. Observing the two data sets correlated in time gave a basic confirmation that the lightning data appeared to be well correlated to the two main supercells.

The WDSS-II integration method, while useful for observing both data sets and their temporal evolution, proved to be somewhat difficult to use when attempting to automatically associate lightning flashes with individual storms. The SCIT numbers produced by WDSS-II tended to not remain associated with the same cell as time progressed.

A secondary problem when using the SCIT output from WDSS-II was that the SCIT itself was represented by a single point with some associated parameters. Typically earlier studies have addressed this issue by using an association radius to correlate lightning flash events with SCITs. This method seemed somewhat arbitrary and might sometimes lead to erroneous associations.

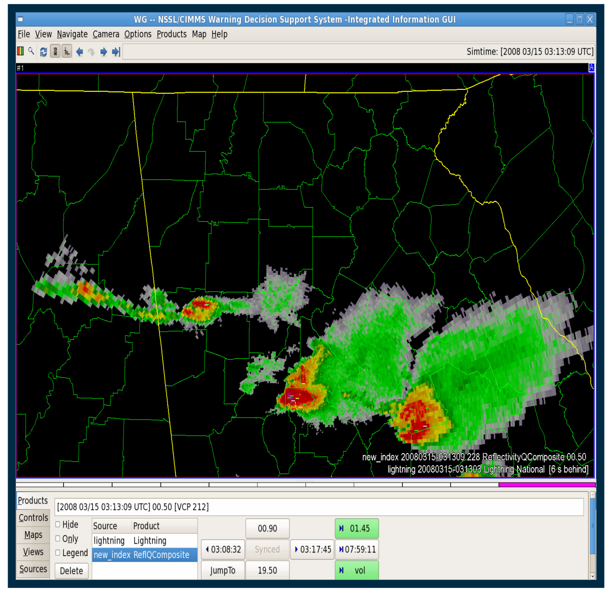

Figure 14. WDSS-II & NLDN Correlation

5.2 SCIT Processing

In an effort to address these concerns, as well as to produce irregularly shaped SCIT areas representative of the radar reflectivity values, a number of adjustments were made to the standard SCIT algorithm. These adjustments were designed to improve its performance in this specific situation, the tracking of several isolated supercells in the area of interest.

First, a set of adjustable criteria for identifying 2-D storm cells (storm cells located in a single elevation slice) was added to increase the probability that a significant storm far from the radar would be properly identified. The increase in vertical distance between sample radar returns increases with range and thus a storm becomes less likely to be detected in multiple elevation slices. The inputs included a required minimum range, minimum mass, and minimum maximum reflectivity factor of the 2-D component.

The second adjustment made to the standard SCIT algorithm involved the discarding of lower reflectivity thresholds. The conventional SCIT algorithm only retains the inner most and highest reflectivity components. Any lower reflectivity component that contains a higher reflectivity component is discarded and the highest reflectivity component is stored. However, the current search method involves searching for any higher reflectivity component that has its azimuth extent within that of the lower reflectivity value and its range extent within its current value. There are cases where this would result in an improper deletion of a storm cell. Thus a distance criterion was used to identify the single component that should be deleted.

The most significant addition to the SCIT algorithm was the creation of a plan view profile of the shape of each SCIT identified. The standard SCIT algorithm only records an estimate of the SCIT region. In the enhanced SCIT processing, a plan view profile was created by taking the union of its individual 2-D components. Furthermore, an option of scaling each 2-D component about its centroid was made available. This allowed for small errors in the location of phenomena that occur near the SCIT perimeter. Once the 2-D components were scaled, the overlapping components were united into a single shape profile. In some cases components did not overlap in the X-Y plane (parallel to Earth's surface). In this case the convex hull of the 2 components was taken including any area between the two components.

5.3 SCIT/NLDN Association

Once the plan profile of each SCIT was created, lightning flashes were spatially associated with the appropriate SCIT. Lightning frequency and types were then plotted versus time. The study was narrowed only to include SCITs detected for an extended period of time, more than 20 consecutive scans, in order to include only the most significant and more developed storm cells.

A plot showing four detected SCITs, three of which were detected for greater than 20 scans, and the lightning flashes associated with each SCIT for a single radar scan is shown in Figure 15. The black 'blob' to the right is the areal SCIT representing the tornadic supercell, while the slightly smaller pink 'blob' to it's immediate left is the areal SCIT representing the second non-tornadic supercell. The third, red 'blob' farther to the left represents a smaller trailing thunderstorm. The small yellow '+' signs within each 'blob' indicate the reported location of individual NLDN flashes.

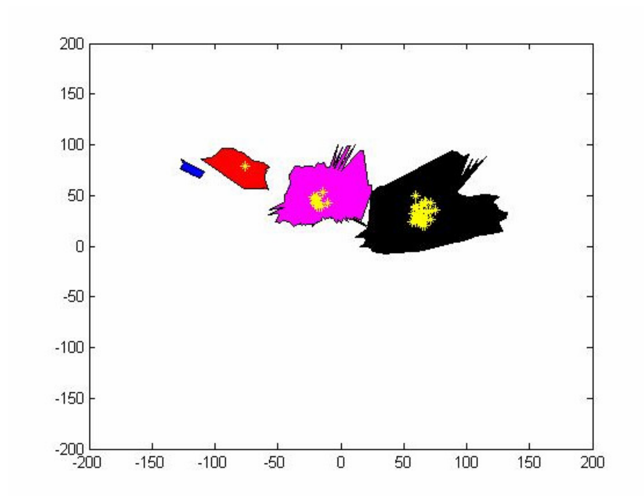

Figure 15. MATLAB SCIT / NLDN Association

6 RESULTS

The MATLAB based SCIT tracking routine followed 3 cells, the tornadic supercell, the non-tornadic supercell, and a third smaller cell, over more than 20 NEXRAD scans as they moved across the state of Georgia. Lightning flash data with locations which corresponded to each of these three cells was collected and analyzed. These analyses are presented below. In each of the plots, the non-tornadic cell is represented by a blue line, the tornadic cell is represented by a green line, and the smaller trailing cell is represented by a red line. In each plot, the radar scan number which most closely corresponded to the time of reported tornado touchdown is indicated by a filled triangle on the green, tornadic cell line.

6.1 SCIT Maximum Reflectivity

In Figure 16, the maximum reflectivity, in dBZ, is plotted for all three cells as a function of radar scan number. The two larger supercells, plotted in blue and green, show similar levels of maximum reflectivity, while the small cell, plotted in red, initially showed a significantly lower maximum reflectivity level. No significant change in maximum reflectivity within the tornadic or non-tornadic SCIT areas can be seen corresponding to tornado genesis or touchdown.

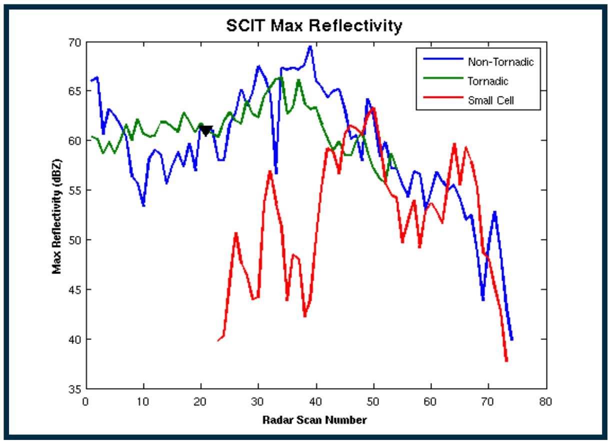

Figure 16. SCIT Maximum Reflectivity

6.2 Total Flash Rates

CG lightning has been associated with tornadogenesis, with peaks in CG rates observed prior to tornado formation and a relative decrease in conjunction with touchdown (Perez, et. al, 1997). Similar “lightning jumps” have been found for “total lightning”, the combination of CG and CC lightning within a storm (Goodman, et al. 2005). It is now thought that the lightning jump prior to the formation of the tornado may be related to the strong updrafts found during this stage of storm development (Deierling 2008a, 2008b). Initial work to characterize the lightning jump phenomenon has shown some correlation to severe weather events and may be used with spaceborne detection of total lightning on the Geostationary Lightning Mapper (GLM) (Schultz 2008).

Total flash rate, as used in this study, is the combined rate of CG and CC flashes detected within each SCIT area during each radar scan interval. A plot of this flash rate for each of the three cells studied is shown below in Figure 17. The plot for the large, tornadic supercell shows a larger overall rate for this storm cell. The tornadic cell total flash rate also shows a significant reduction just prior to tornado touchdown. This is followed by a significant increase shortly after touchdown.

There seem to be at least one other large dip in total flash rate for this cell later in its lifecycle unrelated to the tornado. The second, non-tornadic cell also shows a smaller, but still distinct, dip in total flash rate at almost the same time as the dip was observed in the tornadic cell. The overall rate of total flashes is significantly smaller for the other two, non-tornadic cells.

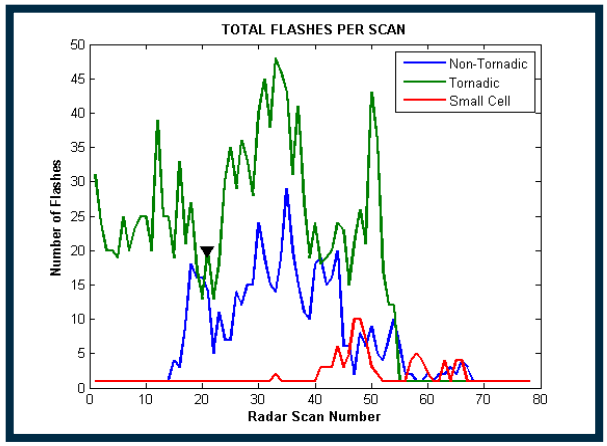

Figure 17. Total Flash Characteristics

6.3 CG and CC Flash Rates

Figures 18 and 19 below show CG and CC flashes detected within each SCIT as a function of radar scan number. There are interesting differences between the two figures. The CG rate for the tornadic cell starts at a relatively high rate and decreases slowly to a more moderate level. The non-tornadic cell exhibits a similar moderate level throughout its lifecycle. The smaller cell shows a much lower CG flash rate than either of the two supercells.

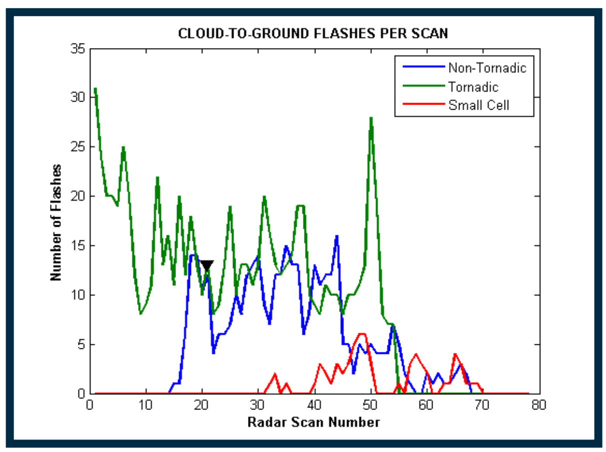

Figure 18. CG Flashes per Scan

Figure 19, depicting the CC flashes within each SCIT, exhibits significant differences between the non-tornadic and the tornadic supercells. The tornadic cell CC flash rate is much higher than the non-tornadic rate over the entire lifetime of the storms, although some of this difference may be due to the difference in areal extent of the two SCITs. Additionally, the tornadic cell shows a dramatic decrease in CC rate just prior to and during tornado touchdown. Both supercells show increases in CC rates in the middle portions of the storm evolution.

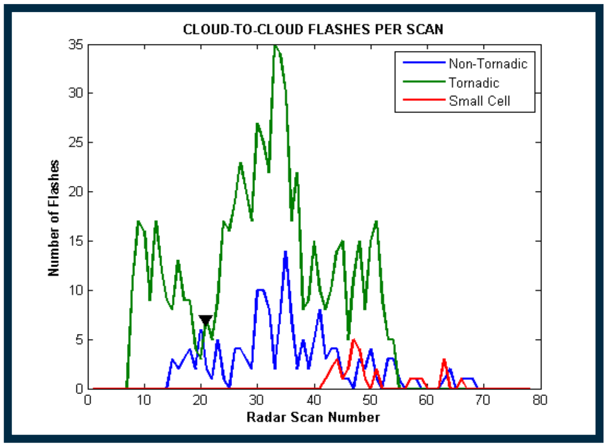

Figure 19. CC Flash Rates

6.4 Positive and Negative Flash Rates

Another aspect of the lightning characteristics examined was the difference between positive and negative polarity flash rates between the three cells. In both of the figures below, the CC and CG flashes are combined and only the polarity of the flash is used to differentiate the events.

Figure 20 shows the number negative flashes associated with each SCIT as a function of radar scan number. While a possible dip in the number of negative flashes may have occurred for the tornadic cell, the data is rather noisy and similar dips can be seen at other times as well. Generally, the negative flash rate for both supercells looks similar, while the small cell shows a much lower rate.

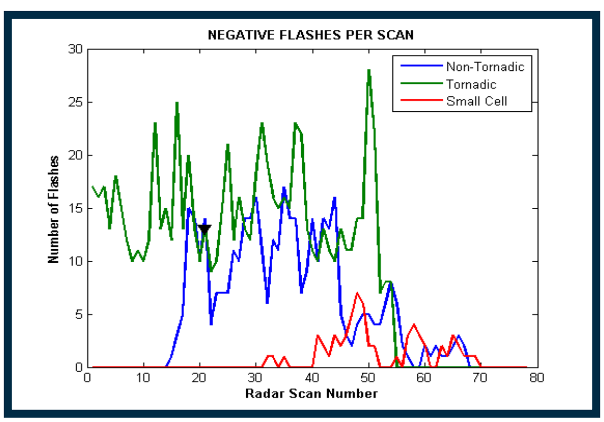

Figure 20. Negative Flash Rates

The positive combined CG and CC flash rate for the three cells is shown in Figure 21. In this case, the tornadic cell again shows a much higher rate than the other two cells. Additionally, the tornadic cell flash rate decreases immediately prior to touchdown and then exhibits a dramatic increase after touchdown.

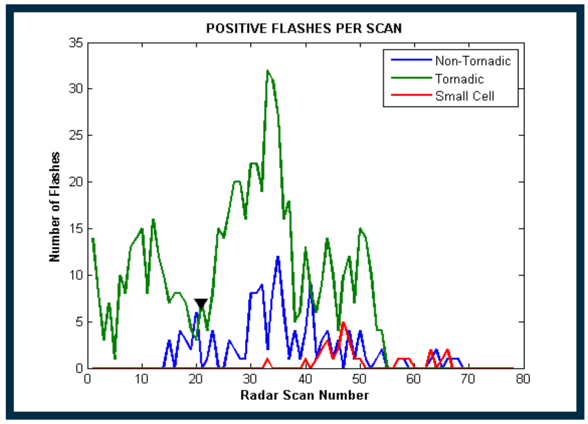

Figure 21. Positive Flash Rates

6.5 Mean Flash Magnitudes

The mean flash magnitude for all type of flashes, both CC and CG and both negative and positive, occurring within each SCIT area plotted as a function of radar scan number is shown in Figure 22. The mean flash magnitude for the tornadic cell appears, in general, to be lower than the mean magnitudes for the other two cells. There may be some indication of a small increase in magnitude for the tornadic cell just prior to and during tornado touchdown, followed by a longer period of lower magnitudes.

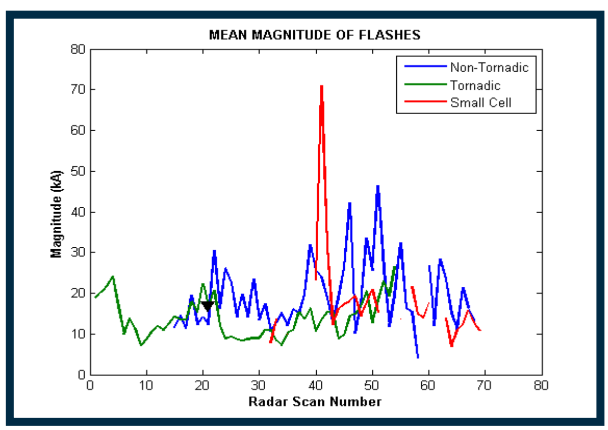

Figure 22. Mean Magnitude of Flashes

7 CONCLUSIONS

This event was characterized more by the “cool season” scenario for tornadic development in the southeastern United States. The storms developed late in the evening as relatively low-topped supercells in an environment with only modest CAPE (just above 1000 J/kg). A critical factor in the development of the storms was adequate low level moisture and a large amount of vertical speed shear, with a 0-3 km SRH over $200m^2/s^2$.

The association of the NLDN flash data with the SCITs showed interesting differences between the two large supercells. The tornadic cell had a significant decrease in both CC and positive flashes just prior to and during the tornado touchdown. There were some differences in overall rates between the tornadic and non-tornadic storms, with the tornadic storm having generally larger rates of both positive and CC flashes. Some of the difference in overall rates could be due to some differences in cell size.

Ongoing work in this area should result in improvements in the SCIT algorithm and better association with the NLDN data. Areas being explored include using more robust methods of special clustering for SCIT determination and temporal correlation for SCIT tracking. Additionally, normalization of the NLDN data by SCIT volume will be included.

8 REFERENCES

Davies, Jonathan M., 2006: RUC Soundings with Cool Season Tornadoes in “Small” CAPE Settings and the 6 November 2005 Evansville, Indiana Tornado. *Extended Abstracts*, 23rd Conference on Severe Local Storms, Amer. Meteor. Soc., St. Louis, MO, 4.3.

Guyer, Jared L. and Imy, David A., 2006: Cool Season Significant (F2-F5) Tornadoes in the Gulf Coast States. *Extended Abstracts*, 23rd Conference on Severe Local Storms, Amer. Meteor. Soc., St. Louis, MO, 4.2.

Rauber, Robert M., John E. Walsh, and Donna J. Charleviox., 2005: *Severe & Hazardous Weather: An Introduction to High Impact Meteorology*. Second Edition. Kendall Hunt Publishing Company.

Wasula, Alicia C., Lance F. Bosart, Russell Schneider, Steven J. Weiss and Robert H. Johns, 2004: Cool Season Tornadoes in the Southeast United States: A Climatological and Case Study Perspective. *Extended Abstracts*, 20th Conference on Severe Local Storms, Amer. Meteor. Soc., Seattle, WA, 16.4.

Lakshmanan, V., T. Smith, G. J. Stumpf, and K. Hondl, 2007: The warning decision support system - integrated information (WDSS-II). *Weather and Forecasting*, 22, No. 3, 592-608.

Lakshmanan, V., A. Fritz, T. Smith, K. Hondl, and G. J. Stumpf, 2007 : An automated technique to quality control radar reflectivity data. *J. Applied Meteorology*. vol. 46 no. 3, pages 288-305

Johnson, J.T., P.L. MacKeen, A. Witt, E.D. Mitchell, G.J. Stumpf, M.D. Eilts, and K.W. Thomas, 1998: The Storm Cell Identification and Tracking Algorithm: An Enhanced WSR-88D Algorithm. *Wea. Forecasting*, 13**,** 263–276.

A.H. Perez, L.J. Wicker, and R.E. Orville, “Characteristics of Cloud-to-Ground Lightning Associated with Violent Tornadoes,” *Weather and Forecasting*, vol. 12, Sep. 1997, pp. 428-437.

Goodman, S. J., R. Blakeslee, H. Christian, W. Koshak, J. Bailey, J. Hall, E. McCaul, D. Buechler, C. Darden, J. Burks, T. Bradshaw, and P. Gatlin, 2005: The North Alabama Lightning Mapping Array: Recent severe storm observations and future prospects. *Atmos. Res.*, 76, 423-437.

Deierling, W., W. A. Petersen, J. Latham, S. Ellis, and H. Christian, 2008a: The relationship between lightning activity and ice fluxes in thunderstorms, *Journal of Geophysical Research*, 113, p. D15210.

Deierling, W. and W.A. Petersen, 2008b: Total lightning activity as an indicator of updraft characteristics, *Journal of Geophysical Research*, 113, p. D16210.

Schultz, Christopher J. and Walter A. Peterson, 2008: The Utility of Lightning Jumps in Severe Thunderstorms in the Tennessee Valley, *Extended Abstracts*, Third Conference on Meteorological Applications of Lightning Data, Amer. Meteor. Soc., New Orleans, LA, P2.3